

Speckle noise reduction in digital holography with spatial light modulator and nonlocal means algorithm

Junmin Leng (冷俊敏)^{1,2*}, Xinzhu Sang (桑新柱)¹, and Binbin Yan (颜纷纷)¹

¹State Key Laboratory of Information Photonics and Optical Communications, Beijing University of Posts and Telecommunications, Beijing 100876, China

²School of Information and Communications, Beijing Information Science and Technology University, Beijing 100032, China

*Corresponding author: junminleng@sohu.com

Received December 26, 2013; accepted March 5, 2014; posted online April 4, 2014

An integrated method based on optical and digital image processing is presented to suppress speckle in digital holography. A spatial light modulator is adopted to introduce random phases to the illuminating beam. Multiple holograms are reconstructed and superimposed, and the intensity is averaged to smooth the noise. The adaptive algorithm based on the nonlocal means is designed to further suppress the speckle. The presented method is compared with other methods. The experimental results show that speckle reduction is improved, and the proposed method is effective and feasible.

OCIS codes: 030.6140, 090.1995, 100.2000.

doi: 10.3788/COL201412.040301.

Digital holographic display has many noticeable advantages such as three-dimensional (3D) display without special eye wears, flexible recording and reproduction and so on. However, most objects are rough on the scale of an optical wavelength in the real world. When a continuous-wave laser illuminates a “random” roughness of the object surface, various microscopic facets of the rough surface devote randomly phased elementary contributions to the total observed field and speckle generates^[1]. The quality of the reconstructed image in the digital hologram is seriously degraded by speckle. Various optical methods and digital algorithms were presented to reduce the speckle. With a slowly moving diffuser associated with a motionless diffuser, the speckle noise was suppressed^[2]. Kang used a rotating mirror to change the incident angle of illuminating beam, and multiple off-axis Fresnel holograms were used to reduce speckle noise by averaging the reconstructed intensity fields. Because of the limit of the rotation range of the mirror, the application field was limited^[3]. Many off-axis holograms were recorded using a circularly polarized illumination beam and a rotating linearly polarized reference beam^[4]. The speckle noise in the reconstruction was suppressed by averaging these fields. Nomura *et al.* utilized different wavelengths to record digital holograms and superposed the reconstruction images to improve the quality of reconstruction images^[5]. The mean filtering and the median filtering were commonly used in the image processing to suppress the speckle noise^[6]. However, details such as edges and contours in the image were lost. Multiple fractional Fourier transform was used to realize high-quality three-dimensional holographic display^[7]. A considerable series of kinoforms (up to 100) were generated and superposed to reduce the speckle noise. Maycock *et al.* adopted discrete Fourier filtering to reduce speckle in digital holography^[8]. Electronic speckle pattern interferometry (ESPI) filtering method was presented based on coherence diffusion and

Perona-Malik diffusion^[9]. The second-order oriented partial differential equation (SOOPDE) filtering model with adaptive selective parameters was used to remove speckle noise^[10]. Other digital filtering methods were developed for denoising, such as Lee filter^[11], Kuan filter^[12], Frost filter^[13] and so on. The nonlocal means (NLM) filter was used for speckle denoising recently^[14].

Here, a method combining optical and digital image processing is presented to suppress speckle noise. Firstly, a spatial light modulator (SLM) is used to introduce random phases to the illuminating light. Multiple holograms with random phases are generated. The intensity superposing and averaging of multiple reconstruction images are used to smooth speckle noise and keep details of the object. Then, a digital image processing algorithm based on NLM is designed and used to further suppress the speckle. The performance parameters of the proposed method are calculated and compared with ones of other methods commonly used.

The speckle is a kind of noise dependent on signal. The phases of speckle are uniformly distributed on the interval $(-\pi, \pi)$, and the intensity is a negative exponential probability density^[1]. When a SLM is used to generate random phases α_l ($l = 1, 2, \dots, L$) that are added into the illuminating beam, multiple holograms are recorded by a charge coupled device (CCD) or complementary metal oxide semiconductor (CMOS) camera.

$$H(x, y; t) = H_1(x, y; t_1) \exp[-i(\varphi_1 + \alpha_1)] + H_2(x, y; t_2) \cdot \exp[-i(\varphi_2 + \alpha_2)] + \dots + H_L(x, y; t_L) \cdot \exp[-i(\varphi_L + \alpha_L)], \quad (1)$$

where $H_1(x, y; t_1)$, $H_2(x, y; t_2)$, \dots , and $H_L(x, y; t_L)$ are the holograms recorded by the camera at different time t_1, t_2, \dots , and t_L , and $\varphi_1, \varphi_2, \dots$, and φ_L are phases of holograms. Multiple images are reconstructed with various patterns of speckle according to the Fresnel transformation method. These different speckle patterns are

uncorrelated with each other and statistically independent. Multiple reconstructed images are superposed and averaged to suppress the speckle noise because this process increases the signal-to-noise ratio (SNR) from 1 to $L^{1/2}$ [15].

The experimental setup is shown in Fig. 1. A 532-nm diode pumped solid state laser with the output power of 50 mW is used. The output light beams are filtered by a pinhole filter. The lens is utilized to transform the filtered light beams into plane light beams. The plane beams are split into the illumination beam and the reference beam by a beam splitter (the ratio of the splitting beams is 7:3). The phase-only SLM (PLUTO-VIS, Holoeye, Germany) is used to digitally generate random phases to add into the illumination beam. The reflected light of the object and the reference light are mixed with a beam splitter whose ratio of the splitting beams is 5:5, and the interference fringes are sampled by a CMOS camera (DH-HV3103UC). The pixel array of the camera is 2048×1536 and the pixel pitch $3.2 \mu\text{m}$. A cubic dice with width of 8 mm is used as the object. The distance between the object and the camera is 408 mm.

The SLM controlled by a computer generates L random phases, and L ($L = 1, 2, \dots, 40$) holograms are obtained for reconstruction. The performance parameter Speckle Index (SI) is used to evaluate the denoising effect. SI of the reconstructed image is defined as^[16]

$$\text{SI} = \frac{1}{MN} \sum_{i=1}^M \sum_{j=1}^N \frac{\sigma(i, j)}{\mu(i, j)}, \quad (2)$$

where M , N are the dimensions of the image. $\sigma(i, j)$ and $\mu(i, j)$ are the standard deviation and the mean value of the $p \times q$ neighborhood of the reconstructed image point (i, j) . p and q are defined as 7 pixels in the proposed method. SI can be regarded as an average reciprocal of SNR, wherein the signal is the mean value and the noise is the standard deviation. In general, SI is less than 1.0. The lower the SI is, the stronger suppression ability the method has.

Figure 2 shows the relationship between SI and the number of holograms. The speckle noise in the reconstructed image can be reduced. As the number of holograms used to denoise increases, speckle is suppressed better. When the number of holograms is less than 6, SI declines considerably and the speckle noise is suppressed quickly and effectively. With further increase in the number, the declining rate of SI is slowed and the values of SI remain basically flat. That is to say, improvements in speckle noise suppression are not very noticeable at a certain point.

The index Equivalent Number of Looks (ENL) is calculated using the following equation^[17]:

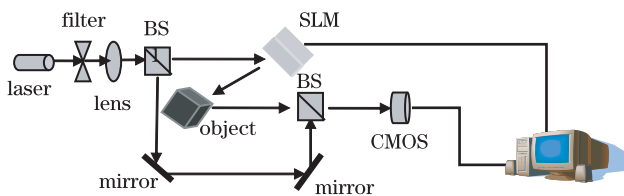


Fig. 1. Optical setup. BS: beam splitter; SLM: spatial light modulator.

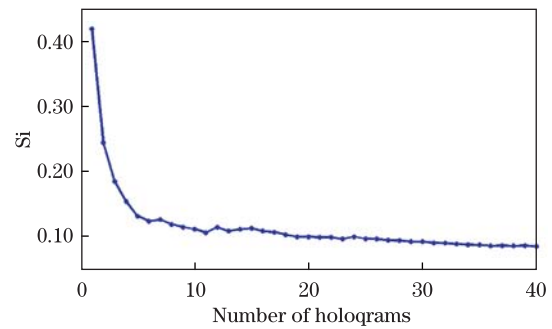


Fig. 2. Relationship of SI and the number of holograms.

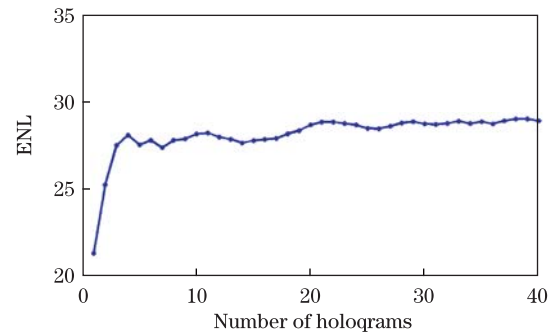


Fig. 3. Relationship of ENL and the number of holograms.

$$\text{ENL} = \left(\frac{\text{mean}}{\text{std}} \right)^2, \quad (3)$$

where mean and std denote the mean and standard deviation of the image. The higher value of ENL, the higher efficiency there is in smoothing speckle noise over homogeneous areas. In the reconstructed image, two homogeneous areas are selected to compute the index ENL as shown in red rectangular zones in Fig. 4(a). Figure 3 shows the relationship between ENL and the number of holograms. When the signal basically keeps constant, the standard deviation is reduced because of the noise suppression, and ENL is increased. ENL rapidly improves as the increasing number of holograms L ($L < 5$), and the effect of smoothing noise is noticeable. When L is further increased, ENL increases slowly. From the Figure 3, we can see that the overall trend of ENL value is the rise and speckle is denoised.

The images from superimposing and averaging reconstruction images of 6, 40 holograms are shown in Figs. 4(b) and 4(c), respectively. Even though 40 holograms are used to suppress speckle, there is speckle noise in the reconstructed image to a certain degree. In view of the quality of the reconstructed images and the above performance indices, we adopt 6 holograms with random phases, and superimpose and average the intensity of the 6 reconstructed images to suppress the speckle noise firstly.

Averaging the intensity of the image over L independent holograms alters the character of the multiplicative speckle noise statistics. As L increases ($L \geq 4$), the speckle probability density function approaches the limit of a Gaussian distribution^[18].

NLM algorithm proposed by Buades *et al.*^[19] uses redundant similarities in an image to remove noise while

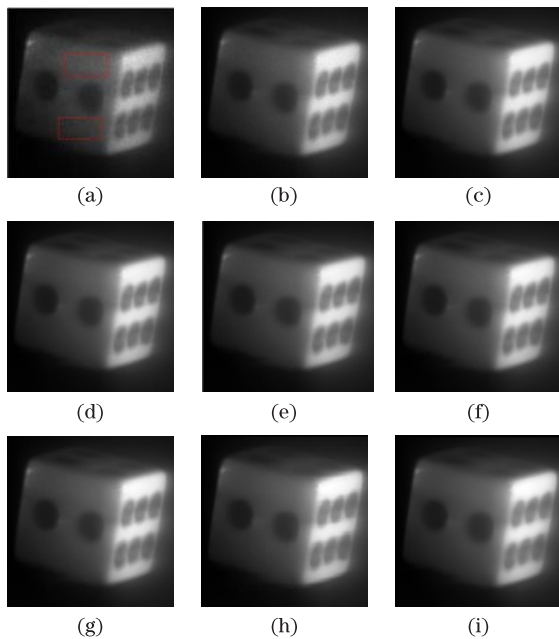


Fig. 4. Reconstructed images. (a) Directly reconstructed image without denoising (red rectangular zones are the selected homogeneous area), (b) and (c) respectively reconstructed from 6, 40 holograms, (d) denoised with median filter, (e) denoised with mean filter, (f) denoised with Kuan filter, (g) denoised with Frost filter, (h) denoised with NLM in Ref. [14], (i) denoised with the proposed method.

preserving textures, and it is one of state-of-the-art denoising methods. NLM algorithm is for images contaminated by Gaussian white noise with zero mean and variance σ_n^2 . Unlike most existing algorithms which mainly rely on local pixels within a small neighbor, NLM algorithm estimates the gray value of a pixel by the weighted average of the gray values of all pixels in the image. The denoised pixel value is

$$u(x_i, y_i) = \sum_{x_j, y_j \in \Omega} w(i, j) v(x_j, y_j), \quad (4)$$

where the weight $w(i, j)$ depends on the similarity between the pixels (x_i, y_i) and (x_j, y_j) , $v(x_j, y_j)$ is the gray value of the pixel (x_j, y_j) and Ω is the image space. The weight satisfies the conditions

$$0 \leq w(i, j) \leq 1 \quad \text{and} \quad \sum_j w(i, j) = 1. \quad (5)$$

The similarity between two pixels (x_i, y_i) and (x_j, y_j) is the similarity of the intensity gray level vectors $v(N_i)$ and $v(N_j)$, where N_k ($k = i, j$) represents a square neighborhood of fixed size and centered at a pixel k . The weight is calculated as

$$w(i, j) = \frac{1}{Z(i)} \exp \left[- \frac{\|v(N_i) - v(N_j)\|_{2, \alpha}^2}{h^2} \right], \quad (6)$$

where $Z(i)$ is the normalizing constant

$$Z(i) = \sum_j \exp \left[- \frac{\|v(N_i) - v(N_j)\|_{2, \alpha}^2}{h^2} \right],$$

$\|v(N_i) - v(N_j)\|_{2, \alpha}^2$ denotes the gray level Euclidean distance between the window of interest and the similarity window, convolved with a Gaussian kernel with parameter α (the standard deviation of the Gaussian kernel $\alpha > 0$). The parameter h acts as a degree of filtering and controls the decay of the exponential function. In the case of Gaussian noise, h^2 is closely related to the noise variance. In Ref. [19], the parameter h was fixed to $12\sigma_n$.

NLM was applied to suppress speckle noise in Ref. [14]. Because the speckle intensity is dependent on the local signal, the parameter h was considered to depend on the pixel to be filtered. The weight is given by^[14]

$$w(i, j) = \frac{1}{Z(i)} \exp \left[- \frac{\|v(N_i) - v(N_j)\|_{2, \alpha}^2}{v(N_j)^{2r}} \right], \quad (7)$$

where r is a noise factor depending on the imaging system parameters. Its nominal value is 0.5.

Here the particularity of speckle noise and the effect of the parameter h on the denoising performance are considered. The parameter h^2 is tuned to the local noise variance. The standard deviation of local noise is estimated by the median of the absolute deviations (MAD) as

$$\hat{\sigma}_{ni} = \frac{1}{0.6745} \text{median}_{x_i, y_i \in \Omega} [|v(N_i)|]. \quad (8)$$

The parameter h is set to be

$$h = 10\hat{\sigma}_{ni}. \quad (9)$$

Therefore, the weight $w(i, j)$ is

$$w(i, j) = \frac{1}{Z(i)} \exp \left[- \frac{\|v(N_i) - v(N_j)\|_{2, \alpha}^2}{(10\hat{\sigma}_{ni})^2} \right]. \quad (10)$$

NLM algorithm adapts the above denoising process for each pixel and outperforms conventional algorithms. However, it takes excessive operation time. Therefore, a large search window replaces the whole image to calculate the weight. To further lower the computational cost and accelerate NLM, on the one hand we adopt the Euclidean distance to compare two pixels to avoid the convolution

$$\begin{aligned} S(i, j) &= \|v(N_i) - v(N_j)\|^2 \\ &= \sum_{l=0}^{W-1} \sum_{m=0}^{W-1} [v_i(l, m) - v_j(l, m)]^2, \end{aligned} \quad (11)$$

where $v_i(l, m)$ and $v_j(l, m)$ represent the pixels $v(x_i, y_i)$ and $v(x_j, y_j)$ in the similarity window, respectively. On the other hand, similar neighborhoods have the same mean and the same gradient orientation. The computation of the gradient orientations is very sensitive to noise and thus requires robust estimation techniques. So the pre-selection of pixels is based on the mean and the variance of $v(N_i)$ and $v(N_j)$. The map of local means and local variances are pre-calculated and stored to avoid repetitive calculations for the same neighborhood. Therefore, the weight becomes

$$w(i, j) = \begin{cases} \frac{1}{Z(i)} \exp \left[-\frac{||v(N_i) - v(N_j)||^2}{(10\hat{\sigma}_{ni})^2} \right], & \text{if } u_1 < \frac{\overline{v(N_j)}}{v(N_i)} < u_2 \text{ and } \sigma_1^2 < \frac{\text{var}[v(N_j)]}{\text{var}[v(N_i)]} < \sigma_2^2. \\ 0, & \text{otherwise} \end{cases} \quad (12)$$

Table 1. Performance Comparison between the Direct Reconstruction, the Reconstruction from 6 Holograms, the One from 40 Holograms, Median Filter, Mean Filter, Kuan Filter, Frost Filter, NLM in Ref. [14], and the Proposed Method

	1 holo.	6 holo.	40 holo.	Median	Mean	Kuan	Frost	NLM	Proposed
SI	0.4181	0.1245	0.0859	0.0865	0.0847	0.0753	0.0751	0.0602	0.0597
ENL	21.242	27.759	28.904	28.114	28.961	29.109	29.114	31.699	31.706

A large size of the search window is chosen as 35×35 pixels and the size of the similarity window is 7×7 pixels ($W=7$) in our algorithm. u_1 is set to 0.9, u_2 is to 1.1, σ_1 0.5 and σ_2 1.5. The reconstructed images are displayed in Fig. 4. The image is directly reconstructed from one hologram according to the Fresnel transformation method in Fig. 4(a). The images in Figs. 4(b) and 4(c) are results from superimposing and averaging reconstruction images of six holograms ($L=6$) and forty holograms ($L=40$), respectively. The reconstruction image from six holograms is further denoised by other filters. The images in Figs. 4(d)–4(g) are results from the median filter, the mean filter, the Kuan filter and the Frost filter. The sizes of the search window and of the similarity window for NLM filter in Ref. [14] are the same with the ones of our algorithm, and the denoised image is shown in Fig. 4(h). The result of the proposed method is in Fig. 4(i). We can see that all of methods can suppress the speckle. Moreover, the reconstruction image of the proposed method is much clearer when compared with other methods. A comparison among these methods in terms of the above two metrics is shown in Table 1.

From Table 1, it can be seen that the proposed method provides better results in terms of SI and ENL, and the advantage of the proposed method relative to the other methods is apparent. Experiments are done on a PC with Intel Core 2 Duo CPU at 2.53 GHz. The computation times are 1.6, 1.4, 12.8, 15.6, 827.6, and 468.4 s for median filter, mean filter, Kuan filter, Frost filter, NLM in Ref. [14] and the proposed algorithm, respectively.

To confirm the proposed method, a dime with a diameter of 19 mm is adopted as the object. The image reconstructed from one hologram is shown in Fig. 5(a) and there is such speckle that the quality of the image is bad. Figure 5(b) is the result of suppression speckle with

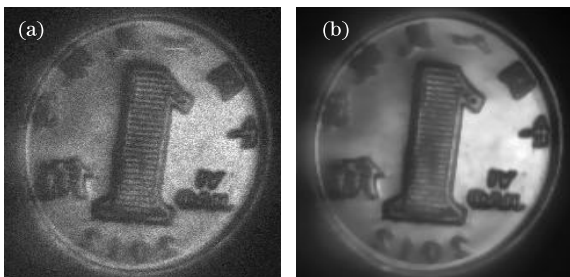


Fig. 5. Another experimental results: (a) noisy image and (b) denoised image.

the proposed method, where six holograms are used to reconstruct the dime. The intensity of six reconstructed images are firstly superimposed and averaged, and then the NLM algorithm is used to further denoise. The denoised image is more vivid than the original noisy image.

In conclusion an integrated method based on optical and digital image processing is presented for suppressing speckle noise. Random phases generated by SLM are added into the illuminating beam. Multiple holograms resulted from multiple random phases are utilized to denoise and reconstruct the image firstly. An adaptive digital algorithm based on the nonlocal means is designed to further suppress the noise. The performance parameters are calculated and compared with ones of other known filters. Experimental results show that the presented method is superior to other methods, and it is effective and feasible for suppressing speckle noise in the digital holography.

This work was supported by the National Natural Science Foundation of China (No.61177018), the Program for New Century Excellent Talents in University (No.NECT-11-0596), the Key Program of Beijing Science and Technology Plan (No.D121100004812001), and Beijing Nova Program (No.2011066). We thank the editor and reviewers for their valuable advice for the improvement of this letter.

References

1. J. W. Goodman, *Speckle Phenomena: Theory and Applications* (Roberts & Company, 2006).
2. S. Lowenthal and D. Joyeux, *J. Opt. Soc. Am.* **61**, 847 (1971).
3. X. Kang, *Chin. Opt. Lett.* **6**, 100 (2008).
4. L. Rong, W. Xiao, F. Pan, S. Liu, and R. Li, *Chin. Opt. Lett.* **8**, 653 (2010).
5. T. Nomura, M. Okamura, E. Nitani, and T. Numata, *Appl. Opt.* **47**, D38 (2008).
6. J. Garcia-Sucerquia, J. A. H. Ramirez, and D. V. Prieto, *Optik* **116**, 44 (2005).
7. H. Zheng, Y. Yu, T. Wang, and L. Dai, *Chin. Opt. Lett.* **7**, 1151 (2009).
8. J. Maycock, B. M. Hennelly, J. B. McDonald, Y. Frauel, A. Castro, B. Javidi, and T. J. Naughton, *Opt. Soc. Am. A* **24**, 1617 (2007).
9. Z. Xiao, Z. Xu, F. Zhang, L. Geng, J. Wu, Q. Yuan, and J. Xi, *Chin. Opt. Lett.* **11**, 101101 (2013).
10. Z. Xiao, Q. Yuan, F. Zhang, J. Wu, L. Geng, Z. Xu, and

- J. Xi, *Chin. Opt. Lett.* **11**, 121201 (2013).
11. J. S. Lee, *IEEE Trans. Pattern Anal. Machine Intell.* **2**, 165 (1980).
 12. D. T. Kuan, A. A. Sawchuk, T. C. Strand, and P. Chavel, *IEEE Trans. Pattern Anal. Machine Intell. PAMI* **7**, 165 (1985).
 13. V. S. Frost, J. A. Stiles, K. S. Shanmugan, and J. C. Holtzman, *IEEE Trans. Pattern Anal. Machine Intell. PAMI* **4**, 157 (1982).
 14. U. Amitai, R. Yair, and S. Adrian, *Appl. Opt.* **A195** (2013).
 15. D. T. Kuan, A. A. Sawchuk, T. C. Strand, and P. Chavel, *IEEE Trans. Acoustics, Speech and Signal Processing* **3**, 373 (1987).
 16. P. Dewaele, P. Wambacq, A. Oosterlinck, and J. L. Marchand, *IGRASS* **10**, 2417 (1990).
 17. L. Gagnon and A. Jouan, *Proc. SPIE* **3169**, 80 (1997).
 18. F. J. Martin and R.W. Turner, *INT. J. Remote Sensing* **14**, 1759 (1993).
 19. A. Buades, B. Coll, and J. M. Morel, *Multiscale Model. Simul.* **4**, 490 (2005).